J Mater Sci (2009) 44:3936–3942
DOI 10.1007/s10853-009-3532-6

Ionic liquid-based synthesis of luminescent YVO_4:Eu and YVO_4:Eu@YF_3 nanocrystals

Aksana Zharkouskay · Heinrich Lünsdorf · Claus Feldmann

Received: 9 February 2009 / Accepted: 29 April 2009 / Published online: 19 May 2009

Abstract Luminescent YVO_4:Eu nanocrystals were prepared via an ionic liquid-based synthesis. According to electron microscopy, dynamic light scattering, and X-ray diffraction, the presence of uniform and highly crystalline particles, 12–15 in diameter is validated. As-prepared particles turn out to be nonagglomerated and redispersible. Photoluminescence exhibits characteristic red emission related to Eu^{3+}. Quantum yield of as-prepared YVO_4:Eu (15 mol%) is determined to 17–19%. The quantum yield of as-prepared material increases to 44–46% by establishing an YVO_4:Eu@YF_3 core-shell structure. Since the lattice planes (001) of YVO_4 and (100) of YF_3 match very well, a crystalline YF_3 shell, 1–2 nm in thickness protects the YVO_4 core very efficiently. Besides the significantly increased quantum yield, the presence of a core-shell structure is further evidenced by electron energy loss spectroscopy. Element mapping revealed high intensities of Eu in the inner parts, associated with low peripheral fluorine intensities.

A. Zharkouskay · C. Feldmann (✉)
Institut für Anorganische Chemie, Universität Karlsruhe (TH), Engesserstraße 15, 76131 Karlsruhe, Germany
e-mail: feldmann@aoc1.uni-karlsruhe.de

H. Lünsdorf
Helmholtz-Zentrum für Infektionsforschung GmbH, Inhoffenstraße 7, 38124 Braunschweig, Germany

Introduction

Europium-doped yttrium vanadate as a bulk material is widely used in displays and fluorescent lamps as an efficient red emitting phosphor [1, 2]. As a nanomaterial, YVO_4:Eu is relevant for these issues as well. Additional interest is related to labeling, signaling, and biomedical purposes [3]. Current access to nanoscale YVO_4:Eu is via microemulsion techniques [4, 5] or solvothermal methods [6–9] applying surface-active molecules, e.g., oleic acid, polyvinylpyrrolidone, or phosphonic acids for colloidal stabilization. These approaches result in well-defined nanocrystals, however with the high-molecular-weight stabilizers adhered on the particle surface via strong coordinative bonds. To exclude such stabilizers, hydrothermal methods have been conducted. This, however, leads to YVO_4:Eu colloids that exhibit a comparably broad size distribution and significant aggregate formation [10–14]. In contrast to bulk YVO_4:Eu (with 70% quantum yield), the nanomaterial has been obtained with comparably low quantum yield only. Most investigations, in fact, do not even address the quantum yield [4–7, 10–13]. In general, values of 15–18% are given [8, 9], only once 25% has been reported [14].

Aim of this study is to realize YVO_4:Eu nanocrystals with intense red emission and significantly increased quantum yield. To this concern, two strategies have been involved. First, thermally stable, 'non'-coordinating ionic liquids (ILs) were used as polar, but aprotic dispersants [15–18]. This allows performing the synthesis at temperatures up to 300 °C, establishing a low lattice-allocated defect concentration, and an easy removal of surface-bound IL constituents from the nanoparticles after the synthesis [19–23]. A second general measure to minimize surface-related loss processes is to protect the luminescent core by

a nonluminescent shell. Quantum dots (e.g., CdSe@ZnS) and rare-earth doped phosphates (e.g., $LaPO_4$:Ce,Tb@$LaPO_4$) impressively validate the success of these core-shell structures [24–26].

Experimental section

All chemicals were used as received from the supplier. All preparative work was performed using standard *Schlenk*-equipment with argon as inert gas.

The synthesis of $[MeBu_3N][N(SO_2CF_3)_2]$ as the IL was performed based on a metathesis reaction with tributhylmethylammonium chloride, $[N(CH_3)(C_4H_9)_3]Cl$ and lithium bis(trifluoromethanesulfonyl)imide, $Li[N(SO_2CF_3)_2]$, following a procedure given elsewhere [27].

Synthesis of YVO_4:Eu nanocrystals

One hundred and twenty-nine milligrams (0.425 mmol) $YCl_3 \cdot 6H_2O$ (Chempur, 99.999%), 28 mg (0.076 mmol) $EuCl_3 \cdot 6H_2O$ (Aldrich, 99.999%), and 0.11 mL (0.466 mmol) $VO(O^iPr)_3$ (ABCR, 98%) were dissolved in 1.5 mL of methanol (MeOH) and 10 mL of IL. This first solution was added dropwise to a solution of 110 mg (2.75 mmol) NaOH in 3.5 mL of MeOH and 5.0 mL of IL. Addition was performed over a period of 15 min under vigorous stirring and at a temperature of 50 °C. The resulting orange dispersion was now heated for 90 min at 200 °C. By this treatment, the dispersion turned colorless and was left to cool to room temperature. Thereafter, the suspension was diluted with 20 mL of ethanol (EtOH) to lower the viscosity of the IL. To remove the IL and remaining salts (e.g., NaCl), the nanocrystals were repeatedly centrifuged and washed by redispersion and centrifugation (Sigma 3K30 centrifuge operated for 30 min at 60,000 × *g*). Hence, washing was conducted twice with water and thrice with EtOH. Finally, the collected colorless solid was dried at room temperature in air. For further analytical characterization, the nanocrystals were applied as-prepared or after redispersion in EtOH.

Synthesis of YVO_4:Eu@YF_3 core-shell structures

YVO_4:Eu nanocrystals prepared as given above were first redispersed in 4 mL of MeOH and 10 mL of IL applying ultrasonication. This dispersion was mixed with a solution containing 15 mg $YCl_3 \cdot 6H_2O$ (0.049 mmol) in 1.0 mL of MeOH. Thereafter, a solution of 6 mg (0.105 mmol) $(NH_4)HF_2$ (Sigma-Aldrich, 99.999%) in 2.0 mL of MeOH was added dropwise at a temperature of 80 °C. This dispersion was heated for crystallization to 190 °C. Thereafter, the resulting colorless core-shell particles were again collected by centrifugation, washing by redispersion and centrifugation, and finally dried at room temperature in air.

X-ray powder diffraction (XRD) was conducted with a Stoe STADI-P operating with Ge-monochromatized Cu-K_α radiation.

Scanning electron microscopy (SEM) was conducted on a Zeiss Supra 40 VP, using an acceleration voltage of 12 kV and a working distance of 4 mm. As-prepared samples were redispersed in DEG, deposited by evaporation on a silicon wafer, and sputtered with platinum.

Transmission electron microscopy (TEM) and electron diffraction were performed on a Philips CM 200 ST/FEG (field emission gun) microscope, operating at 200 kV. TEM samples were prepared by spraying of dispersions in DEG on a Lacey-film copper grid. Selected area electron diffraction (SAED) was performed with bundles of particles.

Electron energy loss spectroscopy was done on colloids that were dried from the alcohol solute onto a 30 nm carbon foils supported by reticulum foils. Parallel EELS were recorded for 220 s on the whole of three integration cycles with an integrated energy-filter TEM (LIBRA120, Zeiss) at an emission current of 2 μA, a spectrum magnification of ×100, an illumination aperture of 0.80 mrad and a 90 μm objective aperture. Spectra were background corrected by power-law [28]. Electron spectroscopic imaging (ESI) was done at the same aperture settings and an energy-slit width of 10 eV, background correction was performed, according to the three-window-power-law method.

Dynamic light scattering (DLS) was performed with a Nanosizer ZS from Malvern Instruments. For DLS analysis as-prepared spheres were redispersed in DEG. The particle diameter was measured in DEG suspension applying polystyrene cuvettes.

Infrared spectra (FT-IR) were measured with a Bruker Vertex 70 FT-IR. The samples were measured in KBr pellets with a resolution of 4 cm^{-1}.

Photoluminescence (PL) was recorded with a Jobin Yvon Spex Fluorolog 3 equipped with a 450 W Xe-lamp, an integrating sphere as well as double grating excitation and emission monochromators. The quantum yield of as-prepared nanocrystals were measured by comparison to bulk YVO_4:Eu (5 mol%) as a reference (commercial lamp and display phosphor, particle diameter: 4–8 μm; quantum yield: 70%, source of sample: Leuchtstoffwerk Breitungen, Germany) [29, 30]. Data were recorded at $\lambda_{excitation} =$ 280 nm with identical slit width and band pass. The number of emitted photons was obtained by integrating the emission spectra (575–775 nm) of the nanocrystalline samples and the reference based on normalized identical absorption (280 nm).

Results and discussion

YVO_4:Eu nanocrystals were synthesized applying $[N(Me)(Bu)_3][N(Tf)_2]$ as IL as well as $YCl_3 \cdot 6H_2O$, $EuCl_3 \cdot 6H_2O$, and $VO(O^iPr)_3$ as starting materials. Previous studies—in contrast to bulk YVO_4:Eu typically doped with 5 mol%—have evidenced an Eu^{3+} content of 15 mol% to be most suited [14, 31]. Consequently, this dopant level was applied here, too. For optimal conditions of particle nucleation, the synthesis was performed at 50 °C in a mixture of IL and ethanol as a cosolvent. Role of the cosolvent, on the one hand, is to reduce the viscosity of the IL, and on the other hand, is to increase the solubility of the starting materials. Thereafter, ethanol was evaporated, and the pre-formed YVO_4:Eu nanoparticles were crystallized in the pure IL by heating to 200 °C. Finally, the as-prepared nanocrystals were washed to remove the IL and remaining salts (e.g., NaCl). YVO_4:Eu was obtained as a colorless powder that can be easily redispersed in polar solvents (e.g., water, methanol, ethanol, and diethylene glycol) by sonification.

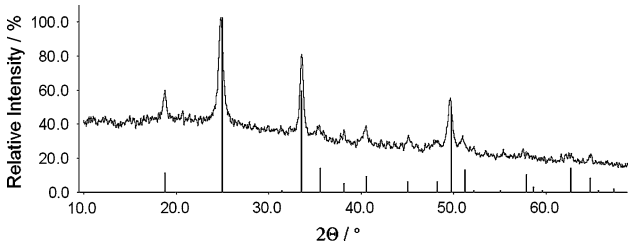

Fig. 1 XRD pattern of YVO_4:Eu nanocrystals (ICDD-No. 17-0341 as a reference)

Composition, purity, and crystallinity of as-prepared YVO_4:Eu nanoparticles are evidenced by XRD (Fig. 1). All Bragg peaks are in accordance to the tetragonal wakefieldite modification. The obvious broadening of the diffraction lines already hints to the presence of nanosized crystals. To this end, a mean crystallite size of 12 nm was calculated applying Scherrer's equation to the most intense Bragg peak ((200) at $2\theta = 25.00°$). Scanning electron microscopy (SEM) was involved to get a closer look at morphology and size (Fig. 2). The nanocrystals turn out to

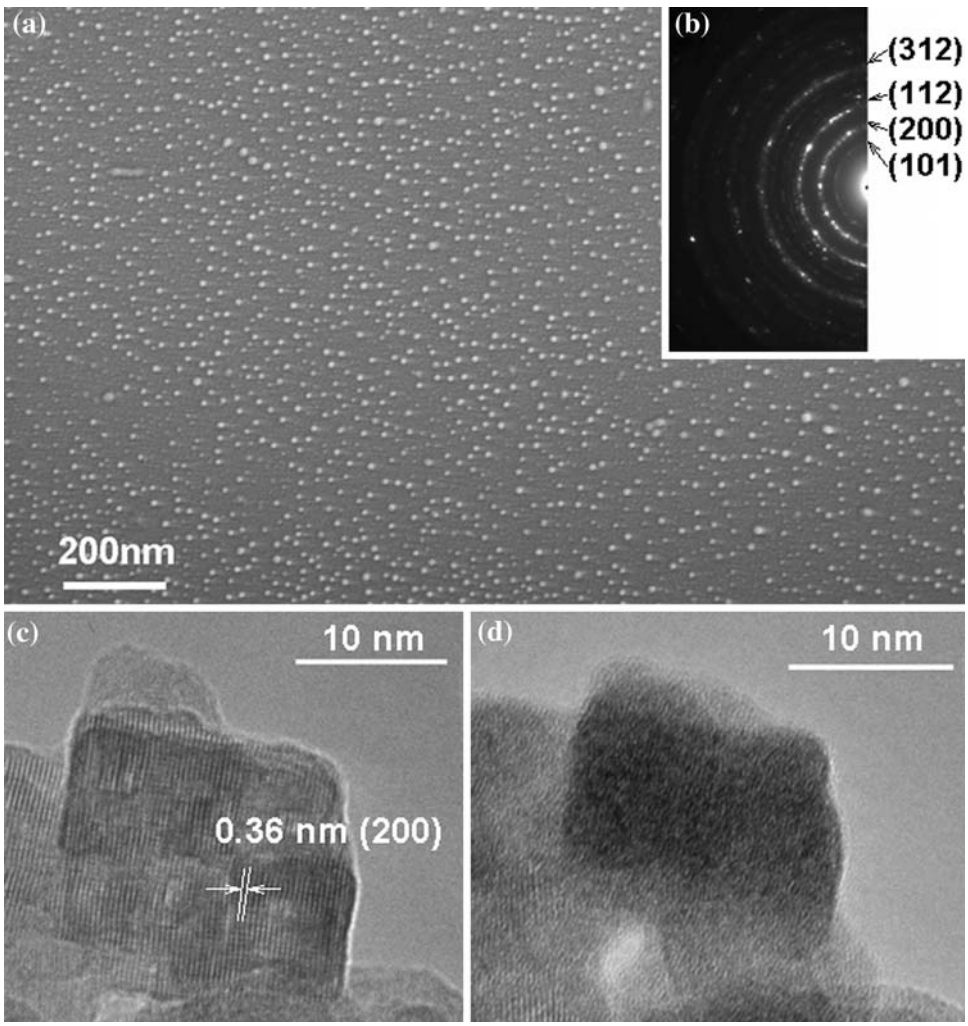

Fig. 2 **a** SEM, **b** SAED, **c** and **d** HRTEM images of as-prepared YVO_4:Eu of a representative nanoparticle, thereof **d** after about 1 min of electron-beam exposure

be nonagglomerated and very uniform in size and shape. The average diameter is deduced to 12–15 nm and consistent with the XRD results. In addition to XRD analysis, which confirms the crystallinity of powder samples, composition and crystallinity of selected individual nanoparticles are evidenced by high resolution transmission electron microscopy (HRTEM) and SAED (Fig. 2). Representative images display YVO_4:Eu nanoparticles with highly ordered lattice fringes, indicating that even areas close to the particle surface are well crystallized. The observed lattice distance is identified as 6.22 Å and corresponds well with (001) (literature data: 6.27 Å) [32]. During HRTEM investigation, the nanocrystals turned out to become amorphous on a minutes time scale (Fig. 2). In fact, such a behavior has been described already and is ascribed to phase separation processes and partial reduction of vanadium [9, 14, 33].

In addition to electron microscopy, the particle size distribution of the title compound was measured in suspension via DLS. To this concern, as-prepared YVO_4:Eu was redispersed in DEG. As a result, an average hydrodynamic diameter of 15 nm, and again a low degree of agglomeration is evidenced (Fig. 3). The colloidal stability of the suspensions is ascribed to charge stabilization of the nanocrystals by the constituents of the IL [34]. Hence, infrared spectra of as-prepared YVO_4:Eu show the characteristic vibrations related to the $[VO_4]^{3-}$ anion as the dominating absorption ($\nu_{(V-O)} = 900–800\ cm^{-1}$) (Fig. 4). On the other hand, the IL ($\nu_{(C-H)} = 2970–2880\ cm^{-1}$, $\nu_{(S-O)} = 1470–1060\ cm^{-1}$) as well as water ($\nu_{(O-H)} = 3500–3300\ cm^{-1}$, $\delta_{(H_2O)} = 1630\ cm^{-1}$) are indeed indicated by weak absorptions [20, 21, 35].

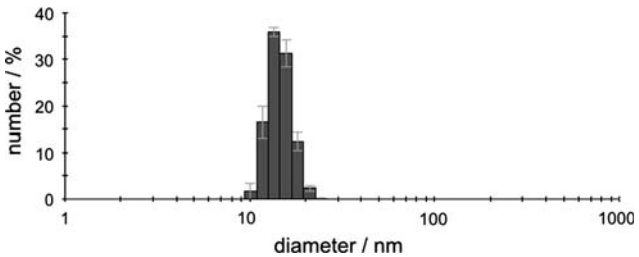

Fig. 3 Particle-size distribution of as-prepared YVO_4:Eu subsequent to washing and redispersion in DEG

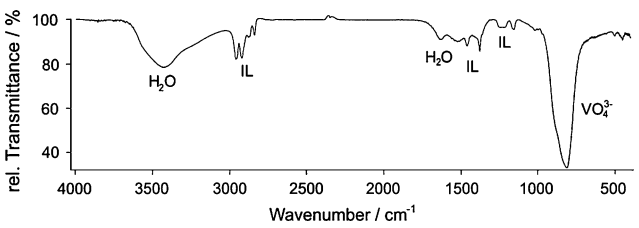

Fig. 4 FT-IR spectrum of YVO_4:Eu nanocrystals

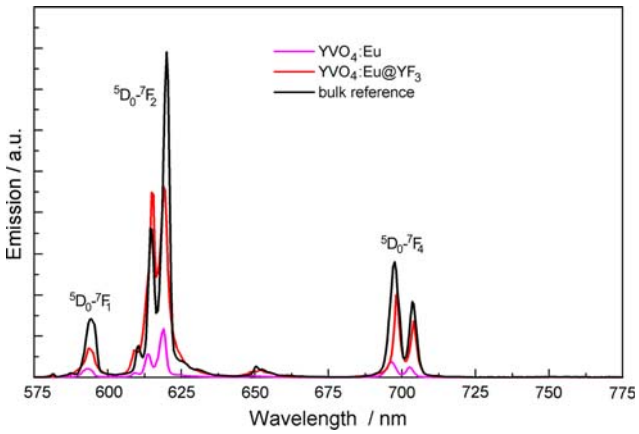

Fig. 5 Emission spectra of YVO_4:Eu (15 mol%) nanocrystals, YVO_4:Eu@YF_3 (15 mol%) nanocrystals and bulk YVO_4:Eu (5 mol%) as a reference ($\lambda_{excitation} = 280$ nm)

Emission spectra of as-prepared YVO_4:Eu (15 mol%) display the characteristic Eu^{3+}-related transitions as described for bulk as well as for nanoscale YVO_4:Eu (Fig. 5) [4–14, 31]. After excitation via (O → V) charge transfer on the vanadate anion and subsequent energy transfer to Eu^{3+}, relaxation occurs due to f–f transitions on Eu^{3+}, with $^5D_0 \rightarrow {}^7F_2$ as the most intense emission line [36, 37]. The quantum yield was determined by comparison to commercial YVO_4:Eu, which is used as an industrial display phosphor. This reference material consists of particles, 4–8 μm in diameter and has been specified with a quantum yield of 70% [28, 29]. Based on normalized absorption of sample and reference, by comparing the resulting emission intensity, a quantum yield of 17–19% is obtained for as-prepared YVO_4:Eu nanocrystals. This value is in good agreement to literature data [8, 9, 14].

Aiming at an increased quantum yield—similar to semiconductor-type quantum dots—a core-shell structure would be most likely in order to decrease surface-related loss processes [24–26]. To guarantee a sufficient lattice matching at the solid–solid interface, the nonluminescent shell is preferentially established by the same compound as the core—or at least a material with almost identical lattice parameters. Since $[VO_4]^{3-}$ as a luminescent center is an intrinsic part of the lattice [31], nondoped YVO_4 is excluded from being a suitable shell. Selection of a shell material is restricted even further due to the anisotropy of the YVO_4 unit cell. The situation is unraveled here by introducing YF_3 as a shell. In general, fluorides are well known for efficient defect healing of oxide materials [38]. Moreover, at least two lattice parameters of YVO_4 ($a = b = 7.10$ Å; $c = 6.27$ Å) are very close to YF_3 ($b = 6.85$ Å; $a = 6.35$ Å) [32, 39]. HRTEM images indeed show a single crystalline YVO_4:Eu core, 12–15 nm in size, which is covered by a highly crystalline YF_3 shell, 1–2 nm in thickness (Fig. 6). The resulting core-shell particles

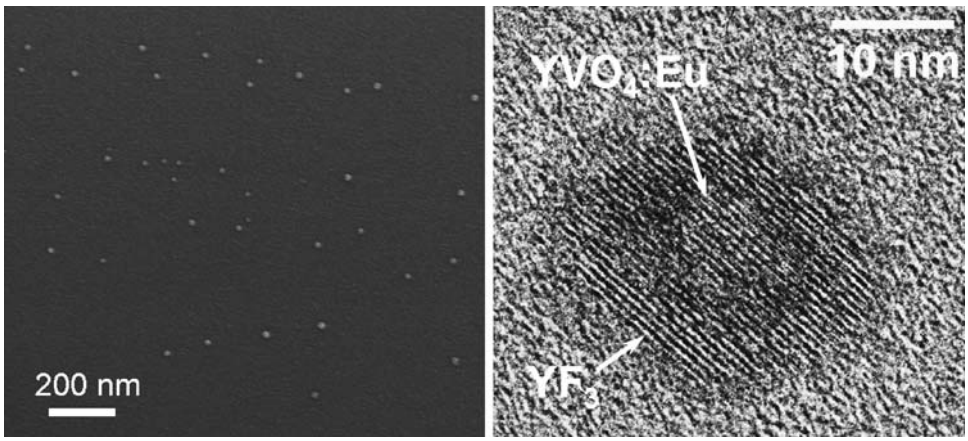

Fig. 6 Overview SEM and HRTEM image of YVO_4:Eu@YF_3 core-shell nanoparticles, with YVO_4 core (001) = 6.22 Å and YF_3 shell (100) = 6.39 Å

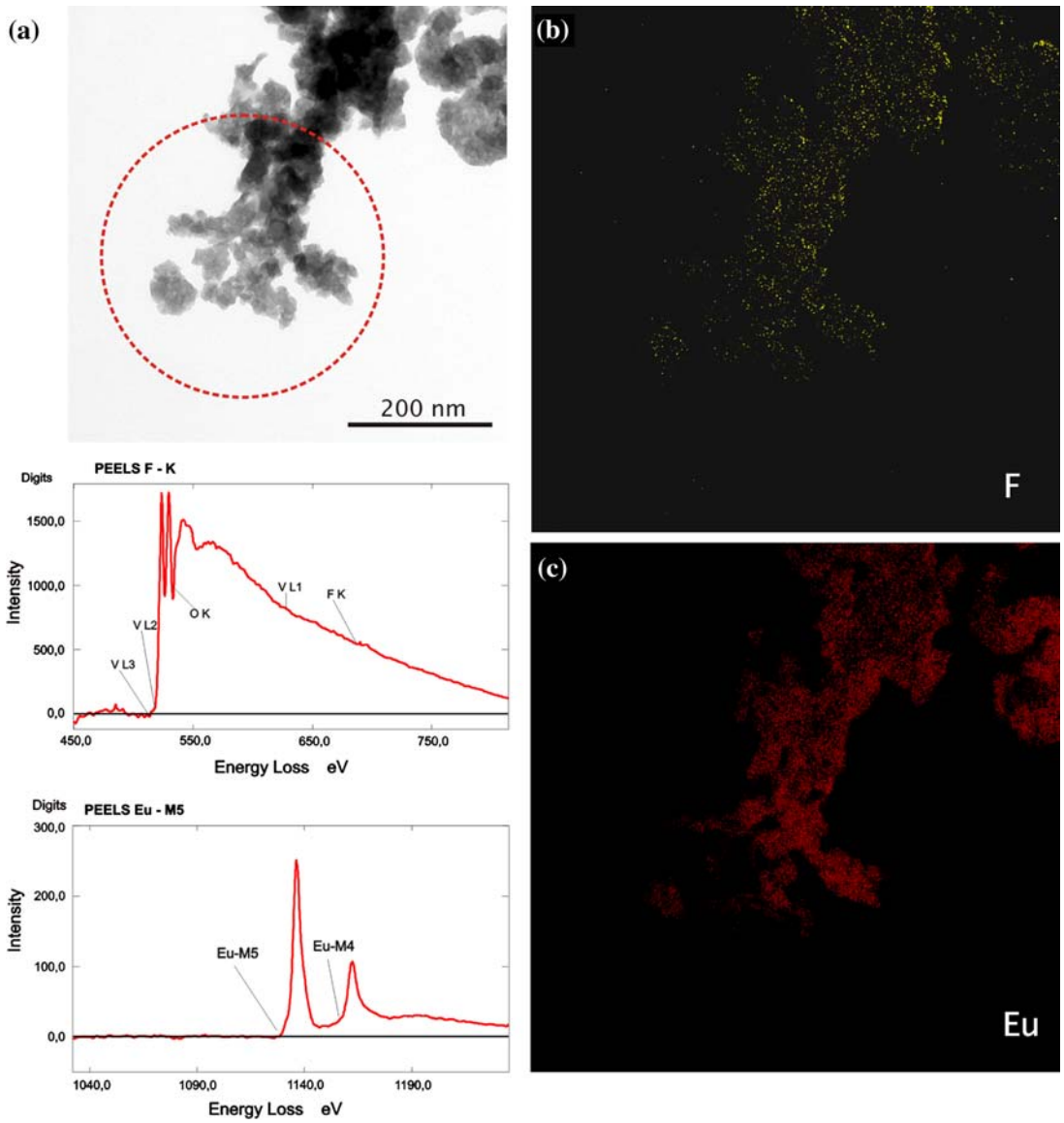

Fig. 7 Electron-energy loss spectroscopy (EELS) of YVO_4:Eu@YF_3 colloid: **a** Bundles of nanoparticles adsorbed to a carbon-foil. Encircled area indicates the PEELS measuring area of the adjacent spectra, which were background corrected. **b** and **c** ESI-maps of F and Eu show their elemental distribution, strictly correlated with the particle bundles

amount to 14–17 nm in diameter and show a sufficient matching between (001) lattice fringes of YVO_4 (measured: 6.22 Å) and (100) fringes of YF_3 (measured: 6.39 Å) [32, 39]. Although electron microscopy indicates the presence of a shell, these investigations are quite complicated due to the low stability of YVO_4 and its alteration when exposed to the electron beam. Standard analytical tools, e.g., DLS and XRD, are—as expected—of very limited reliability due to the low overall amount of YF_3. On the other hand, fluorescence spectroscopy is a very valuable evidence for the core-shell structure (see below). In addition, electron-energy loss spectroscopy (EELS) clearly validates the presence of fluorine throughout the sample (Fig. 7). Here, element mapping reveals high intensities of Eu in the inner parts of the nanoparticles, associated with low peripheral fluorine intensities. According to the Eu:F intensity ratio, the amount of fluorine can be deduced to about 1–3%, which is in agreement to the expectation.

If core-shell structures are established with a sufficient lattice matching of core and shell, a significant increase in quantum yield can be expected [24–26, 38]. Indeed, suspensions of YVO_4:Eu@YF_3 exhibit strong emission of red light even in ethanol (Fig. 8). Emission spectra exhibit a strong increase in intensity when comparing YVO_4:Eu@YF_3 and YVO_4:Eu (Fig. 5). Note that crystal field splitting of $^5D_0$–$^7F_2$ transitions results in a certain change of the emission ratio. The quantum yield of YVO_4:Eu@YF_3 (15 mol%) was recorded again—as described above—by comparing to commercial YVO_4:Eu (5 mol%) as a reference. As a result, a value of 44–46% is obtained.

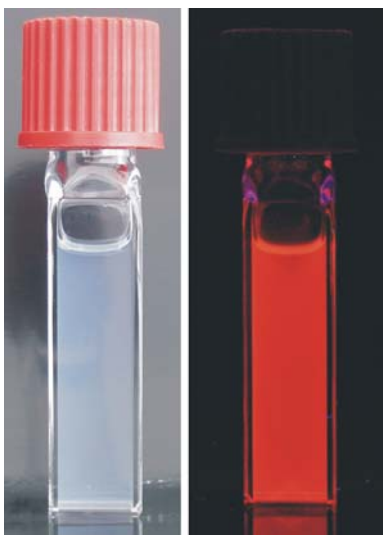

Fig. 8 Dispersion of YVO_4:Eu@YF_3 nanocrystals: nonexcited and with UV-excitation ($\lambda_{excitation}$: 254 nm; solid content: 2.0 wt% in ethanol; opaque appearance due to the use of a flashlight (*left*) and light emission (*right*))

Both results—the emission spectra as well as the quantum yield—are in accordance with a significant reduction of surface-allocated defects, and thereby confirm the presence of the core-shell structure.

Conclusions

In summary, YVO_4:Eu nanocrystals as well as YVO_4:Eu@YF_3 core-shell structures showing intense emission of red light were obtained. The synthesis in ILs results in almost monodispersed, nonagglomerated, and redispersible nanocrystals, 12–15 nm in size. Particle size and size distribution have been consistently measured based on several independent analytical tools. While protecting the luminescent core with YF_3, the quantum yield was increased from 17–19% to 44–46%. YVO_4:Eu core and YF_3 shell show a very good lattice matching. Besides the considerable increase in quantum yield, the presence of the core-shell structure is further evidenced by HRTEM as well as by EELS.

Acknowledgements The authors are grateful to Dr. R. Popescu and Prof. Dr. D. Gerthsen for performing TEM analysis. We also acknowledge the DFG Center for Functional Nanostructures (CFN) at the University of Karlsruhe (TH) for financial support.

References

1. Shionoya S, Yen WM (eds) (1999) Phosphor handbook. CRC Press, Boca Raton
2. Feldmann C, Jüstel T, Ronda CR, Schmidt PJ (2003) Adv Funct Mater 13:511
3. Pellegrino T, Kudera S, Liedl T, Munoz Javier A, Manna L, Parak WJ (2005) Small 1:48
4. Althues H, Simon P, Kaskel S (2007) J Mater Chem 17:758
5. Sun L, Zhang Y, Zhang J, Yan C, Liao C, Lu Y (2002) Solid State Commun 124:35
6. Wang F, Xue X, Liu X (2008) Angew Chem 120:920; Angew Chem Int Ed 47:906
7. Liu J, Li Y (2007) Adv Mater 19:1118
8. Riwotzki K, Haase M (2001) J Phys Chem B 105:12709
9. Riwotzki K, Haase M (1998) J Phys Chem B 102:10129
10. Wu X, Tao Y, Song C, Mao C, Dong L, Zhu J (2006) J Phys Chem B 110:15791
11. Xu HY, Wang H, Jin TN, Yan H (2005) Nanotechnology 16:65
12. Yanhong L, Guangyan H (2005) Solid State Chem 178:645
13. Huignard A, Buissette V, Franville AC, Gacoin T, Boillot JP (2003) J Phys Chem B 107:6754
14. Huignard A, Gacoin T, Boillot JP (2000) Chem Mater 12:1090
15. Greaves TL, Drummond CJ (2008) Chem Rev 108:206
16. Weingärtner H (2008) Angew Chem 120:664; Angew Chem Int Ed 47:654
17. Tundo P, Perosa A (2007) Chem Soc Rev 36:532
18. Wasserscheid P, Welton T (eds) (2002) Ionic liquids in synthesis. Wiley-VCH, Weinheim
19. Ding K, Miao Z, Liu Z, Zhang Z, Han B, An G, Miao S, Xie Y (2007) J Am Chem Soc 129:6362
20. Zharkouskaya A, Trampert K, Heering W, Lemmer U, Feldmann C (2008) Europ J Inorg Chem 87:3

21. Bühler G, Feldmann C (2006) Angew Chem 118:4982; Angew Chem Int Ed 45:4864
22. Itoh H, Naka K, Chujo Y (2004) J Am Chem Soc 126:3026
23. Zhou Y, Antonietti M (2003) J Am Chem Soc 125:14960
24. Steckel JS, Zimmer JP, Coe-Sullivan S, Scott NE, Bulovic V, Bawendi MG (2004) Angew Chem 116:2206; Angew Chem Int Ed 43:2154
25. Harrison MT, Kershaw SV, Rogach AL, Kornowski A, Eychmüller A, Weller H (2000) Adv Mater 12:123
26. Kömpe K, Borchert H, Storz J, Lobo A, Adam S, Möller T, Haase M (2003) Angew Chem 115:5672; Angew Chem Int Ed 42:5513
27. Welton T (1999) Chem Rev 99:2071
28. Egerton RF (1975) Phil Mag 31:199
29. Bril A, Wanmaker WL, Broos J (1965) J Chem Phys 43:311
30. Palilla FC, Levine AK (1966) Appl Optics 5:1467
31. Blasse G, Bril A (1970) Philips Techn Rev 31:304
32. Milligan WO, Vernon LW (1952) J Phys Chem 56:145
33. Hansen S, Smith DJ (1987) Electron Microsc Anal 15:1
34. Antonietti M, Kuang D, Smarsly B, Zhou Y (2004) Angew Chem 117:5096; Angew Chem Int Ed 43:4989
35. Weidlein J, Müller U, Dehnike K (1988) Schwingungsspektroskopie. Thieme, Stuttgart
36. Blasse G, Grabmaier BC (1994) Luminescent materials. Springer, Berlin
37. Brecher C, Samuleson H, Lempicki A, Riley R, Peters T (1967) Phys Rev 155:178
38. West AR (1990) Solid state chemistry and its applications. Wiley, Chichester, p 318
39. Cheetham AK, Norman N (1974) Acta Chem Scand A 28:55